

Novel technique for thermal lens measurement in commonly used optical components

Christina Bogan,^{1,*} Patrick Kwee,¹ Stefan Hild,² Sabina H. Huttner,²
and Benno Willke¹

¹Max-Planck-Institut für Gravitationsphysik (Albert-Einstein-Institut) and Leibniz Universität
Hannover, Callinstr. 38, 30167 Hannover, Germany

²SUPA, Institute for Gravitational Research, University of Glasgow, G12 8QQ, UK

*christina.bogan@aei.mpg.de

Abstract: The absorption of light in transmissive optics cause a thermally induced effect known as thermal lensing. This effect provokes an often undesired change of a laser beam transmitted by the optic. In this paper we present a measurement method that allows us to determine thermal lensing in commonly used optical components. The beam influenced by the thermal lens is expanded into the eigenmodes of an optical cavity, and its modal content is analyzed in the eigenbasis of the cavity. The measured quantity depends neither on beam parameters nor on the position of the optical component under investigation. This method allows, to our knowledge, for the first time the direct measurement of the mode conversion coefficient $|\varepsilon_2|$ of the thermal lens.

© 2015 Optical Society of America

OCIS codes: (350.6830) Thermal lensing; (120.3940) Metrology; (120.6810) Thermal effects.

References and links

1. R. G. Beausoleil, E. K. Gustafson, M. M. Fejer, E. D'Ambrosio, W. Kells, and J. Camp, "Model of thermal wave-front distortion in interferometric gravitational-wave detectors. I. Thermal focusing," *J. Opt. Soc. Am. B* **20**, 1247–1268 (2003).
2. A. Marcano, H. Cabrera, M. Guerra, R. A. Cruz, C. Jacinto, and T. Catunda, "Optimizing and calibrating a mode-mismatched thermal lens experiment for low absorption measurement," *J. Opt. Soc. Am. B* **23**, 1408–1413 (2006).
3. R. C. C. Leite, R. S. Moore, and J. R. Whinnery, "Low absorption measurements by means of the thermal lens effect using an He-Ne laser," *Appl. Phys. Lett.* **5**, 141–143 (1964).
4. S. Hild, H. Lück, W. Winkler, K. Strain, H. Grote, J. Smith, M. Malec, M. Hewitson, B. Willke, J. Hough, and K. Danzmann, "Measurement of a low-absorption sample of OH-reduced fused silica," *Appl. Opt.* **45**, 7269–7272 (2006).
5. A. F. Brooks, D. Hosken, J. Munch, P. J. Veitch, Z. Yan, C. Zhao, Y. Fan, L. Ju, D. Blair, P. Willems, B. Slagmolen, and J. Degallaix, "Direct measurement of absorption-induced wavefront distortion in high optical power systems," *Appl. Opt.* **48**, 355–364 (2009).
6. J. D. Mansell, J. Hennawi, E. K. Gustafson, M. M. Fejer, R. L. Byer, D. Clubley, S. Yoshida, and D. H. Reitze, "Evaluating the effect of transmissive optic thermal lensing on laser beam quality with a shack-hartmann wave-front sensor," *Appl. Opt.* **40**, 366–374 (2001).
7. M. Gugliotti, M. S. Baptista, L. G. Dias, and M. J. Politi, "Single-beam interface thermal lensing," *Appl. Opt.* **38**, 1213–1215 (1999).
8. D. Ottaway, J. Betzwieser, S. Ballmer, S. Waldman, and W. Kells, "In situ measurement of absorption in high-power interferometers by using beam diameter measurements," *Opt. Lett.* **31**, 450–452 (2006).

9. J.-P. Bourgoïn, S. Doiron, M. Deveaux, and A. Haché, "Single laser beam measurement of thermal diffusivity," *Appl. Opt.* **47**, 6530–6534 (2008).
10. V. Quetschke, J. Gleason, M. Rakhmanov, J. Lee, L. Zhang, K. Y. Franzen, C. Leidel, G. Mueller, R. Amin, D. B. Tanner, and D. H. Reitze, "Adaptive control of laser modal properties," *Opt. Lett.* **31**, 217–219 (2006).
11. D. Z. Anderson, "Alignment of resonant optical cavities," *Appl. Opt.* **23**, 2944–2949 (1984).
12. P. Hello and J.-Y. Vinet, "Analytical models of thermal aberrations in massive mirrors heated by high power laser beams," *J. Phys. France* **51**, 1267–1282 (1990).
13. N. Lastzka, J. Steinlechner, S. Steinlechner, and R. Schnabel, "Measuring small absorptions by exploiting photothermal self-phase modulation," *Appl. Opt.* **49**, 5391–5398 (2010).
14. For mirrors with high reflectance only a small fraction of the light passes the substrate such that the situation might be different.
15. For BK7 the thermal expansion α is approximately three times larger than the temperature dependence of the refractive index β (dn/dT). As the two effects act on the beam in the same way the two effects add up linearly.
16. W. Winkler, K. Danzmann, A. Rüdiger, and R. Schilling, "Heating by optical absorption and the performance of interferometric gravitational-wave detectors," *Phys. Rev. A* **44**, 7022–7036 (1991).
17. H. Kogelnik and T. Li, "Laser beams and resonators," *Appl. Opt.* **5**, 1550–1567 (1966).
18. C. Bogan, "Stabilized high power lasers and spatial mode conversion," Ph.D. thesis, Gottfried Wilhelm Leibniz Universität Hannover (2013).
19. P. Kwee, F. Seifert, B. Willke, and K. Danzmann, "Laser beam quality and pointing measurement with an optical resonator," *Rev. Sci. Instrum.* **78**, 073103 (2007).
20. A. Abramovici, W. E. Althouse, R. W. P. Drever, Y. Gürsel, S. Kawamura, F. J. Raab, D. Shoemaker, L. Sievers, R. E. Spero, K. S. Thorne, R. E. Vogt, R. Weiss, S. E. Whitcomb, and M. E. Zucker, "LIGO: The Laser Interferometer Gravitational-Wave Observatory," *Science* **256**, 325–333 (1992).
21. P. Fritschel, "Advanced LIGO Systems Design," Technical Report LIGO-T010075-v2, LIGO Scientific Collaboration (2008).
22. G. M. Harry and the LIGO Scientific Collaboration, "Advanced LIGO: the next generation of gravitational wave detectors," *Class. Quantum Grav.* **27**, 084006 (2010).
23. P. Kwee, C. Bogan, K. Danzmann, M. Frede, H. Kim, P. King, J. Pöld, O. Puncken, R. L. Savage, F. Seifert, P. Wessels, L. Winkelman, and B. Willke, "Stabilized high-power laser system for the gravitational wave detector advanced LIGO," *Opt. Express* **20**, 10617–10634 (2012).
24. L. Winkelman, O. Puncken, R. Kluzik, C. Veltkamp, P. Kwee, J. Poeld, C. Bogan, B. Willke, M. Frede, J. Neumann, P. Wessels, and D. Kracht, "Injection-locked single-frequency laser with an output power of 220 W," *Appl. Phys. B* **102**, 529–538 (2011).
25. P. Kwee and B. Willke, "Automatic laser beam characterization of monolithic Nd:YAG nonplanar ring lasers," *Appl. Opt.* **47**, 6022–6032 (2008).
26. Northrup Gruman Space Technology, Synoptics document, "Terbium Gallium Garnet – TGG," <http://www.optoscience.com/maker/northrop/pdf/TGG.pdf>.
27. A. Ashkin, G. D. Boyd, J. M. Dziedzic, R. G. Smith, A. A. Ballman, J. J. Levinstein, and K. Nassau, "Optically-induced refractive index inhomogeneities in LiNbO₃ and LiTaO₃," *Appl. Phys. Lett.* **9**, 72–74 (1966).
28. J. Yao, Y. Chen, B. Yan, H. Deng, Y. Kong, S. Chen, J. Xu, and G. Zhang, "Characteristics of domain inversion in magnesium-oxide-doped lithium niobate," *Physica B* **352**, 294–298 (2004).
29. F. S. Chen, J. T. LaMacchia, and D. B. Fraser, "Holographic storage in lithium niobate," *Appl. Phys. Lett.* **13**, 223–225 (1968).

1. Introduction

A good spatial mode profile with specified waist size and position is essential for high precision applications such as medicine, laser machining or laser interferometry. Furthermore, these applications often require high power laser sources. However increasing the laser power potentially distorts the beam quality due to thermal lensing. Thermal lensing is a rather weak effect with typical focal lengths of more than several kilometers. The power of the thermal lens scales with the optical power and the absorption of the substrate.

The presence of absorption in coatings and substrates in connection with the intensity profile of laser beams causes a non-uniform temperature distribution in optical materials. Their index of refraction is in general temperature dependent. Therefore, the heated component acts on a transmitted beam like a lens [1]. To mitigate potential problems optical materials with low absorption coefficients are preferred in most experiments. Nevertheless, even in these commonly-used, low-absorbing components a thermal lens is present, especially in combination with high

laser powers, but it is hard to measure and quantify precisely.

In principle the thermal lens of a given component could be calculated knowing the beam parameters and the absorption of the component to a high precision. In practise, the beam waist and position can be measured very accurately. However, the exact absorption coefficient of optical components is hard to determine. Given the fact that thermal lensing and absorption are strongly related, a standard method to determine a material's absorption is to measure its thermal lens [2–4]. In literature, there are several known methods to measure thermal lensing: Measuring the change in the radius of curvature with a Shack-Hartmann wave-front sensor [5, 6]; measuring the beam size change either with a high dynamic range CCD camera or using a combination of an iris aperture and a photo diode [2, 3, 7–9]. A third method is the expansion of the beam into cavity eigenmodes [10]. In the eigenbasis of the optical cavity the amount of power in second order modes is the criterion of the mode mismatch of the beam to that cavity [11]. Thus, the power in the second-order modes at the cavity represents a measurement of a thermal lens. We will show that this method allows us to exactly determine the thermal lens of a component, knowing neither the beam parameters, nor the position of the component.

2. Theory

Thermal lenses are the result of laser light being absorbed inside an optical material. In general, this happens in both the coating and the substrate of the transmitted optic. Both effects can be calculated independently [1, 12], but a measurement can seize only the entire component. However in most cases, the amount of power absorbed inside the coating is smaller than inside the substrate as the coating thickness can be neglected compared to the dimensions of the substrate [13]. This holds true for optical components with high transmittance as discussed in this paper [14]. Therefore, we are considering only the absorption inside the substrate in the following.

The absorption of power inside a transparent dielectric material results in heat deposition changing the optical path length through this material. Three mechanisms provoked by a temperature change can occur: temperature dependence of index of refraction, strain dependence of index of refraction and thermal expansion. For a wide range of optical materials the effect of the latter two mechanisms is much smaller than the temperature dependence of the refractive index β (dn/dT) and can be neglected [6, 15, 16]. Hence, in the following only the effect of the temperature dependence of index of refraction is considered.

The thermally induced change of the length of the optical path δs between the center of the beam and the point where the intensity has dropped to e^{-2} for an absorption inside the substrate is [16]:

$$\delta s = \frac{1.3\beta p_a d}{4\pi\kappa} \cdot P, \quad (1)$$

where β is the temperature dependence of the refractive index (dn/dT), κ is the thermal conductivity, p_a is the absorption per unit length, d is the length of the substrate and P is the incident power. The focal length of the corresponding thermal lens can be calculated with

$$f_{\text{thermal}} = \frac{w^2}{2\delta s} = \frac{2\pi\kappa}{1.3p_a\beta d} \cdot \frac{w^2}{P}, \quad (2)$$

where w is the beam radius in the substrate [4]. The refractive power of a lens is defined as $\Phi = 1/f$. The parameter $m_0 := 1.3p_a d \beta / (2\pi\kappa)$ combines the material properties of the substrate, which are assumed to be constant. Therefore the refractive power of a thermal lens of a given substrate varies only with the beam size and the laser power used:

$$\Phi_{\text{thermal}} = m_0 \frac{P}{w^2}. \quad (3)$$

Thermal lenses can be treated as weak, thin lenses [12]. Therefore, the q parameter of a beam passing a thermal lens of power $\Phi = 1/f \ll 1$ changes according to

$$q' = q \frac{1}{1 - \Phi q} \approx q + \Phi q^2 \quad \text{with } q := i z_0 - z, \quad (4)$$

where z_0 is the Rayleigh range of the beam and z is the distance from the waist [17]. The waist size of the beam $w_0(q)$ and its position $z(q)$ are given by (see Eq. (4))

$$w_0(q) = \sqrt{\frac{\Im(q)\lambda}{\pi}}, \quad z(q) = -\Re(q), \quad (5)$$

where λ is the laser wavelength. The transformation of the beam due to the propagation through a thin lens can also be described by a single complex parameter

$$\epsilon_2 := \frac{\delta w}{w_0} + i \frac{\delta z}{2z_0}, \quad (6)$$

where $\delta w/w_0$ describes the relative change of the beam waist and $\delta z/z_0$ the relative change of the waist position. With

$$\frac{\delta w}{w_0} = \frac{w_0(q) - w_0(q')}{w_0(q)} = 1 - \sqrt{1 - 2z\Phi} \approx z\Phi \quad (7)$$

and

$$\frac{\delta z}{z_0} = \frac{z(q) - z(q')}{z_0} = -z_0\Phi + \frac{z^2}{z_0}\Phi \quad (8)$$

the change of the beam after propagating through a weak thin lens can be described by

$$\epsilon_2 \approx z\Phi - \frac{i}{2} \left(z_0\Phi - \frac{z^2\Phi}{z_0} \right) = z_0\Phi \cdot \gamma(z/z_0) \quad (9)$$

$$\text{with } \gamma(x) := x - \frac{i}{2} (1 - x^2) \quad (10)$$

$$\text{and } |\gamma(x)| = \frac{1 + x^2}{2}. \quad (11)$$

Thus, a weak, thin lens placed directly at the beam waist ($x = 0$) has no effect on the waist size but on its position. If the lens is placed one Rayleigh range away from the beam waist ($x = 1$) the waist position will not be affected but the waist size will change.

Combining Eq. (9) with Eq. (3) yields

$$|\epsilon_2| = \frac{1 + x^2}{2} \cdot z_0 \cdot m_0 \cdot \frac{P}{w^2} = \frac{\pi}{2\lambda} \cdot m_0 \cdot P = \frac{2.6 \cdot \beta_{pad}}{8\kappa\lambda} \cdot P. \quad (12)$$

Therefore $|\epsilon_2|$ describes the transformation of a laser beam propagated through a thermal lens independently of the beam parameters or the lens position and is called mode conversion coefficient. $|\epsilon_2|$ depends only on the material of the thermal lens and the beam power. Thus measuring $|\epsilon_2|$ directly reduces measurement errors. In the following we will show that this can be realized by expanding the beam into cavity eigenmodes.

Similar to expressing small misalignments of a beam to an optical cavity in first-order Hermite-Gauss modes, HG₁₀ and HG₀₁, a small mode mismatch of a beam can be expressed

by the second-order Laguerre-Gauss mode LG_{10} using the basis given by the cavity eigenmodes [11]. When the waist position of the input beam has a small axial displacement δz with respect to the fundamental mode of the resonator and its size differs from the waist size of the cavity eigenmode by a small fraction $\delta w/w_0$, the relative power in the second-order LG mode can be calculated using ε_2 (see definition (6)) [11, 18]:

$$\frac{P_{LG_{10}}}{P_{\text{tot}}} = |\varepsilon_2|^2. \quad (13)$$

The relative field strength of the LG_{10} mode can be measured by coupling the beam into a scanning non-degenerate cavity taking advantage of the different resonance frequencies for different order modes. In principle, the LG_{10} mode can be arbitrarily reduced by optimizing the positions of two lenses placed in front of the cavity as long as the input beam resembles the fundamental mode [19]. In reality the reduction of the mode mismatch is limited by the range of focal lengths of lenses usually available in a laboratory, the available space in the optical setup and lens errors. Therefore, in addition to the power dependent mode mismatch created by the thermal lens a static mode mismatch has to be considered as well as light in the LG_{02} mode of the undisturbed test beam. The latter originates from beam ellipticity or astigmatism and cannot be distinguished from the radial symmetric LG_{10} mode in a cavity scan. Thus, only the combined power in second order modes can be measured. Using Eqs. (9), (12) and (13) this leads to [18]

$$\frac{P_2(P)}{P_{\text{tot}}} = |\varepsilon_s + \varepsilon_2|^2 + \frac{P_{LG_{02}}}{P_{\text{tot}}} = |\varepsilon_s|^2 + \frac{P_{LG_{02}}}{P_{\text{tot}}} + \frac{z_0 \cdot m_0}{w^2} (\varepsilon_s \gamma^\dagger + \varepsilon_s^\dagger \gamma) \cdot P + \frac{\pi^2}{4\lambda^2} \cdot m_0^2 \cdot P^2, \quad (14)$$

where ε_s represents the static mode mismatch in analogy to ε_2 . This equation can be written as a quadratic function of P [18]:

$$\frac{P_2(P)}{P_{\text{tot}}} = a_0 + a_1 \cdot P + a_2 \cdot P^2 = a_0 + a_1 \cdot P + |\varepsilon_2|^2. \quad (15)$$

In contrast to a measurement without static mode mismatching there is a dependence on the beam parameters and the position of the thermal lens (see Eq. (14)) which scales with the static mode mismatch. In real experiments the parameters of the beam as well as the positions of the various components cannot be measured with arbitrary accuracy. Therefore, it is useful to reduce the static mode mismatch very carefully for each measurement.

3. Setup and calibration

The measurement of the thermal lens of commonly used transmissive optical components requires high sensitivity as their absorption coefficient is typically rather low. Therefore high laser power is required preferably in pure fundamental mode. For our measurements we chose the output beam of a stabilized high power laser system built for the Advanced LIGO [20–22] gravitational wave detector. An identical copy, so called PSL Reference System [23, 24], delivered about 130 W of laser light at a wavelength of 1064 nm with a fundamental mode content of 99.5 %. Additionally, our measurement took benefit of the highly stable power and frequency of the laser system as frequency and power noise potentially distort the thermal lens measurement.

In Fig. 1 the experimental setup is illustrated. A combination of a motorized half-wave plate and a thin-film polarizer forms an attenuation unit and allows us to adjust the laser power probing the test substrate. A second identical unit attenuates the beam after transmission through the test substrate to an allowable level of 130 mW for the two measurement instruments. A fused silica lens in front of the substrate under test defines the beam parameters inside the substrate.

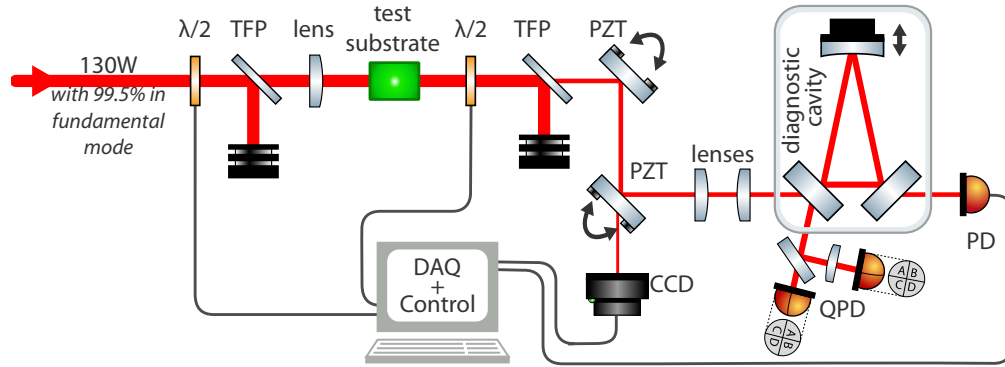


Fig. 1. Experimental setup to measure the thermal lens of a test substrate. DAQ + Control, Data-Acquisition and Control system; PD, photo detector; CCD, camera with high dynamic range; PZT, mirror with piezoelectric element; QPD, quadrant photo diode, TFP, thin-film polarizer.

However, this lens as well as all other transmitted optics used in this experiment should not form a thermal lens on their own. This was verified in a background measurement, where no test substrate was placed in the setup (see Results).

The beam transmitted by the test substrate is coupled into a scanned optical cavity using two piezo actuated mirrors for auto-alignment and two spherical lenses for mode matching. For the alignment control loop, two quadrant photo diodes detected the beam reflected by the cavity at different Gouy phases. The alignment control compensates long-term drifts of the beam position due to environmental temperature fluctuations. The thermal lens measurement was performed using the modescan technique [19] with a tool called diagnostic breadboard as described in [25]. For each power probing the test substrate we recorded the relative transmitted power over a hundred cavity scans and averaged the results.

The cavity scan decomposes the beam into cavity eigenmodes and allows the measurement of the amount of power in the LG_{10} mode. The power dependence of the LG_{10} mode content allows us to deduce the thermal lens of the substrate placed in the setup (see Eqs. (12) and (13)). However, this is masked on the one hand by static mode mismatch and on the other hand by a non zero LG_{02} mode content of the undisturbed measurement beam (see Eq. (14)) as the two second order LG modes have the same resonance frequency. In Fig. 2 a cavity scan is shown in blue, where no test component was placed in the beam path. The beam has a fundamental mode content of more than 99.5 %. A second measurement was performed with an additional optical lens placed in the beam path. The lens had a nominal focal length of 10.83 m and was placed at $x = -5.96 \pm 0.21$. The measured change of the LG_{10} mode content agrees very well with the prediction using Eq. (13) in combination with Eq. (9), even though the measurement cannot differentiate between the LG_{10} mode and the LG_{02} mode.

Additionally, the relative beam size change was measured using a CCD while the power of the beam probing the substrate was changed. A WinCamD-UCD23 (DataRay Inc.) which has a dynamic range of 43 dB was used for the measurements. The CCD was placed in transmission of a mirror with a reflectivity of $R_p = 99\%$ and two neutral density (ND) filters, because the laser power detected by the CCD has to be lower than 10 mW for narrow beams. This method allows us to measure the thermal lens of the test substrate independently. In contrast to the mode decomposition the accuracy of this measurement depends on the knowledge of the beam, the detector position and the substrate position. In principle, it is also possible to pick a position for

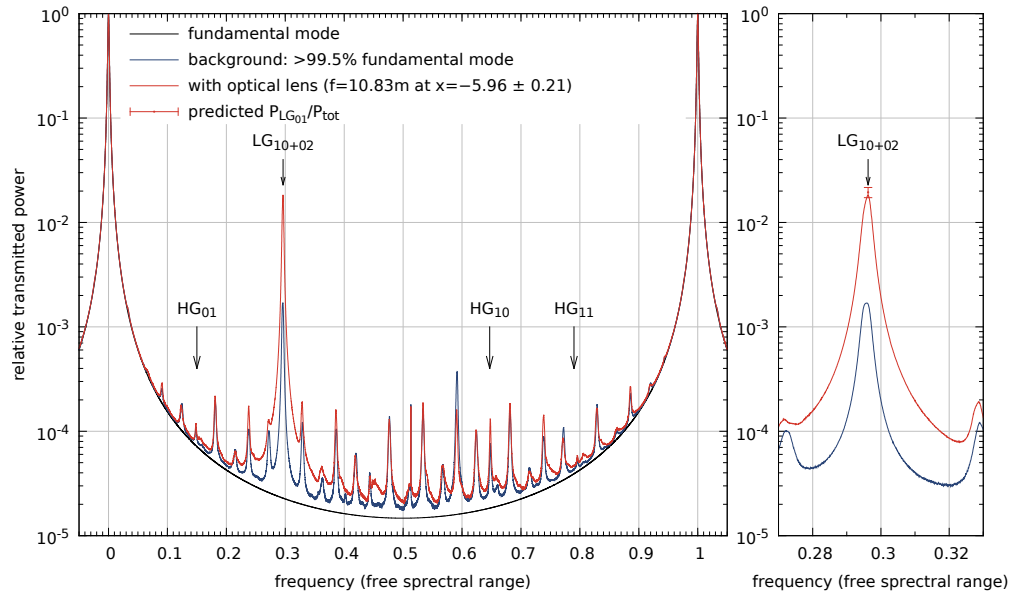


Fig. 2. Cavity scan at a power level of 1 W between the two attenuation units. The positions of the five lowest-order modes are marked according to the free spectral range. A back-ground measurement was performed without a test substrate. A measurement with an additional optical lens in the beam path agrees well with prediction (see Eqs. (9) and (13)).

the detector where the relative beam size does not change in presence of a thermal lens.

Figure 3 shows the measurement of the thermal lens of a N-BK7 wedged laser window with an anti-reflective (AR) coating from Thorlabs (WW11050-C14) performed with cavity scans and the CCD simultaneously. The power of the thermal lens of the N-BK7 window was measured to be $\Phi = 1.3 \cdot 10^{-3} \cdot P / (\text{m} \cdot \text{W})$ for the CCD measurement and $\Phi = 1.25 \cdot 10^{-3} \cdot P / (\text{m} \cdot \text{W})$ for the cavity measurement as a function of the laser power probing the window. The two measurement methods agree within their errors.

A computer system controlled the two half-wave plates in order to adjust the laser power transmitted by the test substrates and recorded the measurement data from the CCD and the mode scan. Therefore, the measurement was operated fully automated once the substrate under test had been placed and the laser beam coupled into the cavity. The power probing the test substrate was increased to the maximum power level in several steps and decreased again. A time span of 150 s between the power change and the cavity scans ensured a fully evolved thermal lens in a steady state. For each power 100 cavity scans were measured and analysed. The relative power in the different modes was detected and the focal length of the thermal lens calculated.

4. Results

The experimental setup allowed a measurement of the thermal lens of several optical components, glasses and crystals. In Fig. 4 the measurement of a polarizing beam splitter (PBS) is shown. The cube had a length of 15 mm and was made of flint glass. The relative mode content of the two second-order LG modes varies quadratically with the power transmitted through the PBS. The content of the first-order modes is stable for the different powers due to the alignment

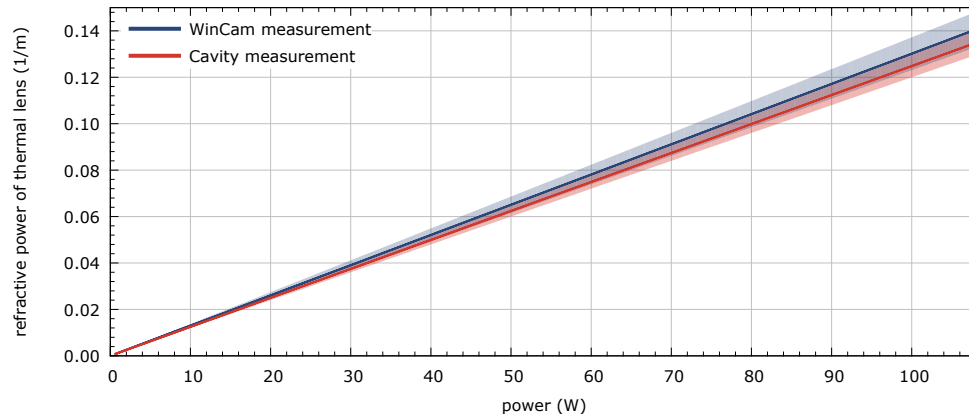


Fig. 3. Power of the thermal lens of a N-BK7 window measured at position $x = 5.03$. The measurement of the relative beam size change was performed with the WinCam. The amount of power in the LG₁₀ mode was measured with the cavity and the thermal lens calculated. Both measurements agree within their errors, which are shown shaded.

control loop. Additionally, a background measurement is shown, where no substrate was placed in the beam path. It is obvious that the various components in the optical setup do not influence the thermal lens measurement.

The relative mode content of the second-order LG modes was fitted using the quadratic function Eq. (15) and the three parameters a_0 , a_1 and a_2 were determined. The parameter a_0 is the sum of the relative power of the LG₀₂ mode and the square of the absolute value of the static mis-mode matching (see Eq. (14)). The square of the absolute value of ϵ_2 is equal to $a_2^2 \cdot P^2$, and was shown to depend exclusively on material parameters (see Eq. (12)). The parameter a_1 is a mixed term of the static mis-mode matching and ϵ_2 . The smaller this parameter a_1 , the less static mode mismatching was observed. The focal length of the thermal lens can be calculated using Eq. (9). The thermal lens of the measured PBS is rather weak with a focal length of $776 \text{ m} \cdot \text{W/P}$. Therefore the thermal lens is hardly noticeable in typical laboratory experiments with laser powers in the order of some watts and optical path lengths of some meters.

We measured the thermal lens of several optical components. The results of these measurements are shown in table 1. For each component the substrate material, length and position x (see Eq. (9)) are listed as well as the beam diameter in the middle of the component and the maximum power used. Additionally, the three parameters that were gained from the fit to the relative mode power of the two second-order LG modes (see Eq. (15)), and the calculated focal length of the thermal lens are shown. All substrates had an AR coating on both surfaces. The tested components were: a N-BK7 window, a PBS (polarizing beam splitter), an acousto-optic modulator crystal (AOM), a LBO (Lithium Triborate [LiB₃O₅]) crystal, a PPKTP (periodically poled potassium titanyl phosphate [PP-KiOPO₄]) crystal, Faraday glass TGG (Terbium Gallium Garnet), a magnesium doped Lithium Niobate crystal [5 mol% Mg: LiNbO₃] (LN) and a Rubidium Titanyl Phosphate crystal [RbTiOPO₄] (RTP).

The AOM crystal had the weakest thermal lens measured with this setup. Its focal length was measured to be $7404 \text{ m} \cdot \text{W/P}$. This corresponds to a relative waist size change of approximately $3 \mu\text{m}$ on the CCD and could not be resolved in our measurements. A PPKTP and a LBO crystal were inserted to the setup as well. Both crystals are commonly used for second-harmonic generation. A thermal lens could not be measured in these two crystals, as the power of the

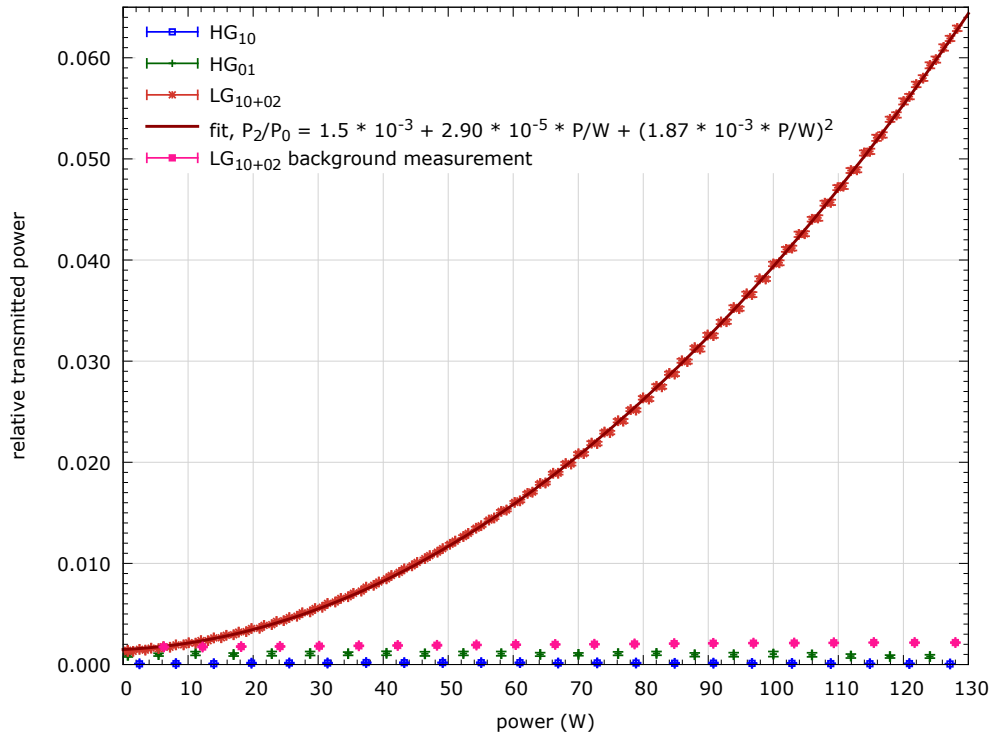


Fig. 4. Thermal lens of a polarizing beam splitter cube made of flint glass: The relative mode content of the two first-order HG modes and the two second-order LG modes is shown as function of the power that was transmitted through the substrate. For comparison a measurement with no test substrate placed in the beam path is shown (background measurement).

second-order LG modes did not change significantly with increased laser power.

For the TGG crystal the thermal lens was measured to have a focal length of $365 \text{ m} \cdot \text{W}/P$. As the material parameters were known for this crystal the absorption per unit length could be calculated:

$$p_a = \frac{4 \cdot \kappa \cdot \lambda \cdot a_2}{1.3 \cdot \beta \cdot d} = 0.00131 \text{ cm}^{-1}, \quad (16)$$

with $\kappa = 7.4 \text{ W}/(\text{m} \cdot \text{K})$, $\lambda = 1064 \text{ nm}$, and $\beta = 20 \cdot 10^{-6} / \text{K}$. This agrees well with the value given in literature for these crystals of $< 0.0015 \text{ cm}^{-1}$ [6, 26].

The measurements that were performed with LN crystals, often used for electro optical modulators (EOM), could not resolve a thermal lens due to the photo-refractive effect [27–29]. For the alternative EOM material RTP we did not observe any photo refractive effect at the intensities used and were able to measure a weak thermal lens.

5. Conclusion

Thermal lensing is caused by the absorption of optical power inside a component and the temperature dependence of the refractive index. Thus, it is fully described by material parameters. However, standard methods to measure the thermal lensing effect rely on the knowledge of the beam parameters and the exact position of the components.

Table 1. Parameter and results of thermal lens measurements of different substrates. The quantity $|\epsilon_2| = a_2 \cdot P$ was shown to depend exclusively on material parameters (see Eq. (12)).

substrate			beam diameter (μm) at center of substrate	max. Power (W)	fitting parameter			focal length ($\text{m} \cdot \text{W}/P$)
material	length (mm)	position x			a_0 (10^{-3})	a_1 (10^{-5})	a_2 (10^{-3})	
BK7 (N-BK7)	5	-5.03	854	108	1.384	1.257	1.347	1031 ± 231
PBS (flint glass)	15	-5.87	991	128	1.485	2.896	1.871	776 ± 25
AOM (TeO_2)	31	-5.49	914	122	0.419	-0.205	0.167	7404 ± 475
LBO (LiB_3O_5)	50	-1.93	170	119	no measurable thermal lens effect			
PPKTP	28	-0.91	111	124	no measurable thermal lens effect			
Faraday (TGG)	40	-6.24	1036	75	1.182	-9.895	4.332	365 ± 11
LN (5 mol% Mg: LiNbO_3)	21	-5.28	887	41	thermal lens not measurable due to photo-refractive effect			
RTP (Y-cut RbTiOPO_4)	40	-5.38	903	133	19.879	0.435	0.445	2722 ± 206

The measurement technique shown in this paper measures directly the mode conversion coefficient $|\epsilon_2|$ of a thermal lens. This parameter was introduced and was shown to depend exclusively on material parameters. An expansion of the beam into the eigenmodes of an optical cavity allows us to measure the mode conversion coefficient directly. The validity of the presented measurement technique was demonstrated by measuring an optical lens. An independent measurement using a CCD camera showed good agreement to the cavity scan method.

Additionally, we measured the thermal lens of several commonly used optical components. The weakest thermal lens had a focal length of $7404 \text{ m} \cdot \text{W}/P$ and was created in an AOM crystal.

Acknowledgment

This research is supported by the Deutsche Forschungsgemeinschaft as a part of the QUEST cluster of excellence and the “Volkswagen Stiftung” (Germany). C.B. acknowledges financial support by the “Hannover School of Lasers, Optics and SpaceTime Research”. The authors acknowledge support from STFC (Grant Ref:ST/L000946/1) and the International Max Planck Partnership (IMPP). S.H. was supported by the European Research Council (ERC-2012-StG:307245).